Spin glass and noninteracting nanoparticle phenomenologies in the same alloy: Magnetic monitoring of the atomic diffusion processes and implications on the microstructure

A. López,* F. J. Lázaro, M. Artigas, and A. Larrea
Instituto de Ciencia de Materiales de Aragón, Universidad de Zaragoza-Consejo Superior de Investigaciones Científicas, 50015 Zaragoza, Spain

(Received 17 July 2001; revised manuscript received 1 August 2002; published 8 November 2002)

The magnetic behavior of a *unique* sample of $Cu_{97.5}Co_{2.5}$ is shown to vary from spin-glass-like, in the as-spun state, towards that of a noninteracting nanoparticle ensemble after sequential annealing treatments. This result is explained by specifically considering the role of the remaining copper-cobalt solid solution regions. In particular a progressive cobalt depletion of the nanoparticle surroundings seems to affect the effectiveness of the Ruderman-Kittel-Kasuya-Yosida interaction mechanism between the Co-rich particles. The presented explanation may also be of help in understanding the magnetic properties of other metallic alloys much beyond the copper-cobalt case.

DOI: 10.1103/PhysRevB.66.174413 PACS number(s): 75.50.Lk, 75.50.Tt, 64.75.+g

I. INTRODUCTION

The magnetic behavior of materials is substantially determined by their microstructure, but the quantitative prediction of this effect is not free from obstacles. However, in the particular case of dilute assemblies of spins or small magnetic particles, the problem is rather simplified because no domain-wall associated magnetization processes have to be considered. These weakly magnetic materials are generally paramagnetic, superparamagnetic, or combinations of both, at room temperature,[1] although the effects of anisotropies and interactions between the submicroscopical magnetic moments may acquire an interesting role on lowering the temperature.

In the last two decades numerous works have analyzed magnetic interaction phenomena among small magnetic entities in the dilute regime, in the research frames of spin glasses[2,3] and magnetic nanoparticles.[4,5] In the presence of interactions, the magnetization dynamics departs from the expected behavior for individual magnetic entities. Eventually, not only the composition, but also the size and the distance between those small entities will influence the magnetic behavior of the system. The concentrated ferrofluids studied by Jonsson *et al.*[6] show typical spin-glass dynamics at low temperatures due to the dipole-dipole interactions, whereas the most diluted are good model systems for superparamagnetism. The parameter that controls the crossover from spin-glass-like behavior (a collective phenomena) to thermally activated dynamics of an ensemble of isolated particles is, in this case, the particle-particle distance.

In the search for model materials for these studies, it looks rather convenient to consider binary alloys, because otherwise the number of possible microstructural phases increases considerably and the problem may become extremely complex. The Cu-Co alloy, at low cobalt content, offers a good example for these studies. Its equilibrium phase diagram shows very little miscibility of cobalt in copper at room temperature,[7] therefore good solid solutions are not stable and can only be prepared by high effective cooling rate methods.[8] Aging, with precipitation of cobalt-rich nanoparticles, can be achieved by controlled annealing of the alloy.[9]

The Cu-Co system has been widely used as a model to study classical nucleation.[10] Precipitation and coarsening in this alloy have been studied by several techniques, which include small-angle neutron scattering, field ion microscopy, transmission electron microscopy, and atom probe techniques.[11] Although many experimental studies have been published on this subject the understanding of the microstructural processes is still an open issue. The great variety of nonequilibrium alloys that can be prepared with the same composition but different preparation methods and, furthermore, with different preparation parameters, is in our opinion a major difficulty to compare results from different experimental studies.

The magnetic properties of Cu-Co alloys have earlier on attracted much attention. For low cobalt content, and depending on the preparation procedures, nearly model superparamagnetism[12–14] or spin-glass behavior[8] has been observed. Giant magnetoresistance is also exhibited in fast cooled Cu-Co samples after suitable annealing treatments.[15] Since the magnetic and magnetotransport properties were proven to be dependent on the thermal treatment parameters, some efforts were devoted to the control of the microstructure.[16] However, at least in the beginning, the alloys were naively considered just as an assembly of magnetic nanoparticles immersed in a conducting but nonmagnetic medium. This assumption may be somehow reasonable if only the most salient phenomena are considered, but is not rigorous in the frame of general basic concepts of alloys. It has been gradually recognized later that several magnetic phases are generally present,[17–20] and that their physical location in the microstructure is at the origin of visible magnetic anomalies.

In spite of the similarities that were suggested early on, the magnetic behavior of spin glasses and noninteracting nanoparticles is today quite well differentiated, the microstructural characterization of the samples being a requirement in any rigorous work. However, although much of the work has been done in both fields independently during the last decades, few works have considered systems in which, by microstructural reasons, both phenomena are present in the same sample, and even less have considered a

correlation between microstructure changes and magnetic properties.

In recent studies on $Cu_{100-x}Co_x$ ($x=2.5,10$), dynamical susceptibility experiments have been used to follow the Co segregation process in melt-spun samples.[19,21] The microstructure and the magnetic properties were jointly interpreted in terms of three Co-containing phases: (i) the fcc Cu-Co supersaturated solid solution (α phase), (ii) the nanometric Co-rich particles (β phase) that grow coherently into the α-phase grains, and (iii) the large Co-rich particles (γ phase) ($\sim$10–100 nm) precipitated at the grain boundaries. In these works it was possible to observe not only the blocking transition of the nanometric β-phase particles and the magnetic contribution of the γ phase, but also the low-temperature anomalies ascribed to the spin-glass freezing of the α phase.

From the previous experiments, it is apparent that the relative contribution of the different phases in as-spun alloys is strongly dependent on the preparation batch, and it is in general poorly reproducible. The sharp magnetic detection of the different phases is hindered by interactions among the microstructural species and this effect increases for increasing cobalt concentration.

In this paper, a magnetic and microstructural study of the changes occurring in the melt-spun alloy $Cu_{97.5}Co_{2.5}$ as result of thermal treatments is presented. In the selection of this sample, we have considered that a higher Co concentration would produce a very complex microstructure in which the microscopical entities would easily interact.[19] In particular, a *unique* sample was chosen among several as-spun products, in order to avoid uncontrolled microstructural dependences on the preparation batch. This sample has been subjected to subsequent thermal treatments and after each annealing period it has been magnetically characterized. As far as we know, this experiment has never been done before and its results clearly suggest that the growth mechanism of the Co-rich particles (β phase) might be connected with the decrease of the magnetic interaction in the thermally treated samples. An interpretation is proposed, based on the influence of the cobalt depletion of the Co-rich nanoparticle surroundings on the effectiveness of the Ruderman-Kittel-Kasuya-Yosida interaction between these particles. A microstructural characterization of the sample at its initial and final states has also been performed by transmission electron microscopy (TEM) to support the interpretation of the magnetic data. Results from other $Cu_{100-x}Co_x$ samples of concentrations $x=2.5$ and 10, previously published,[19,21] have been taken into account in the discussion to illustrate this interpretation.

II. SAMPLE DESCRIPTION AND EXPERIMENTAL TECHNIQUES

The $Cu_{97.5}Co_{2.5}$ alloy was prepared in Ar atmosphere by the conventional melt spinning technique. The liquid alloy was ejected from a quartz crucible onto a rotating wheel with a surface velocity of 50 m/s. A batch of the ribbons obtained in this way was enclosed in a silica glass tube sealed under vacuum and subsequently annealed at 550 °C for 1, 5, and 19 h. After each thermal treatment, the sample was quenched in water at room temperature. It should be noted that, in contrast to other previous studies, *the same sample has been used along this process*. Thus the cumulative annealing times t_a, amount to 1, 6, and 25 hours (labeled $1h$, $6h$, and $25h$, respectively, as stated throughout the paper). Eventually the sample was kept at room temperature on a shelf for 19 months. At the end of this period the sample was analyzed again. In what follows, these characterization data will be labeled as $25h^*$. For the TEM experiments, small pieces of the ribbons were glued onto copper support grids and subsequently argon ion milled at liquid-nitrogen temperatures. The observations were conducted in a Jeol 2000FXII microscope equipped with a Link Analytical energy dispersive spectrometer (EDS).

The dynamical susceptibility and the field-dependent magnetization were measured in a superconducting quantum interference device magnetometer (Quantum Design) equipped with an ac option. The amplitude of the ac exciting field was 0.11 mT and the frequencies used were 1, 10, and 120 Hz.

III. EXPERIMENTAL RESULTS

A. Transmission electron microscopy

The sample both in its as-quenched and in the $25h^*$ state has been characterized by TEM. In Fig. 1(a), a representative region of an intragrain zone of the sample in its as-quenched state is shown. In the micrograph, the dark regions correspond to residual strain fields that are well known in this type of rapidly cooled materials.[22] In Fig. 1(b), a micrograph obtained in bright-field/zone-axis incidence (BFZA) of the sample in the $25h^*$ state is shown. In the picture, ring-shaped strain contrasts, produced by $\sim 6-7$ nm coherent Co particles (β phase), can be observed. According to computer simulations developed by Hattenhauer and Haider[23] for these conditions, the outer region of the dark ring coincides to within ± 0.2 nm with the diameter of the spherical particle. From comparison of Figs. 1(a) and 1(b), and from the complete TEM study of these samples, we should emphasize that no such clearly recognizable ring-shaped contrasts are visible in the as-quenched specimen. In Fig. 2, a typical grain boundary region of the sample in the $25h^*$ state is shown. In the micrograph, larger ($\sim$40 nm) precipitates, marked with arrows in the picture, can be seen at the grain boundary. The composition of these precipitates has been investigated by EDS, clearly indicating their Co-rich nature (γ phase). The comparison of the EDS spectrum of such precipitates with the one obtained from the intragrain zone appears in Fig. 3. Again these intergrain precipitates were not visible in the TEM observation of the sample in the as-quenched state. The results of the TEM characterization of the sample in the as-quenched state, in particular the practical absence of the β and γ species, justify the choice of such sample as a good starting one for the experiment developed in this study.

B. Magnetic characterization

The temperature dependence of the dynamical susceptibility measured at 10 Hz is shown in Fig. 4. As a general rule,

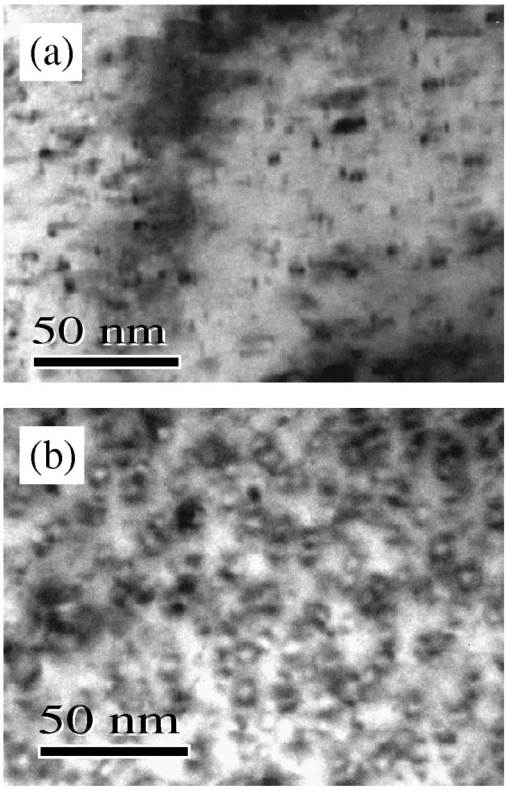

FIG. 1. TEM micrographs of representative intragrain zones of (a) the sample in its as-quenched state, and (b) the sample in its $25h^*$ state. The ring-shaped strain contrasts, produced by $\sim 6-7$ nm coherent Co particles (β phase) in (b) have been obtained by the bright-field/zone-axis incidence [112] (BFZA) technique in order to have a better comparison with the literature data (Ref. 23).

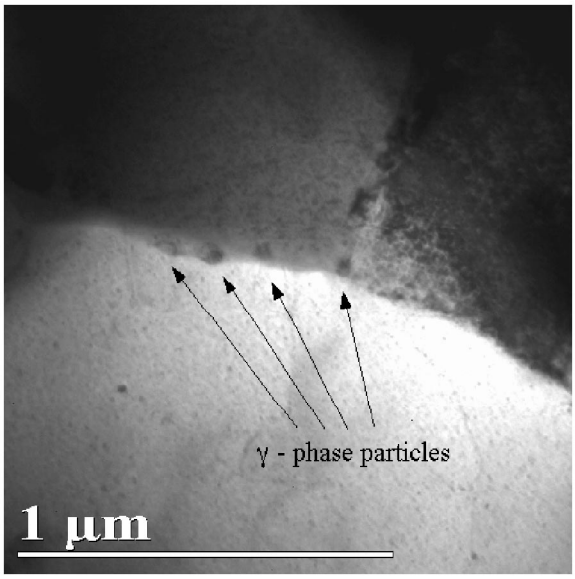

FIG. 2. TEM micrograph of a typical grain boundary region of the sample at the same $25h^*$ state previously shown in Fig. 1. Note the presence (marked with arrows) of particles (γ phase) at the grain boundaries. The composition of these precipitates has been investigated by EDS, as shown in Fig. 3.

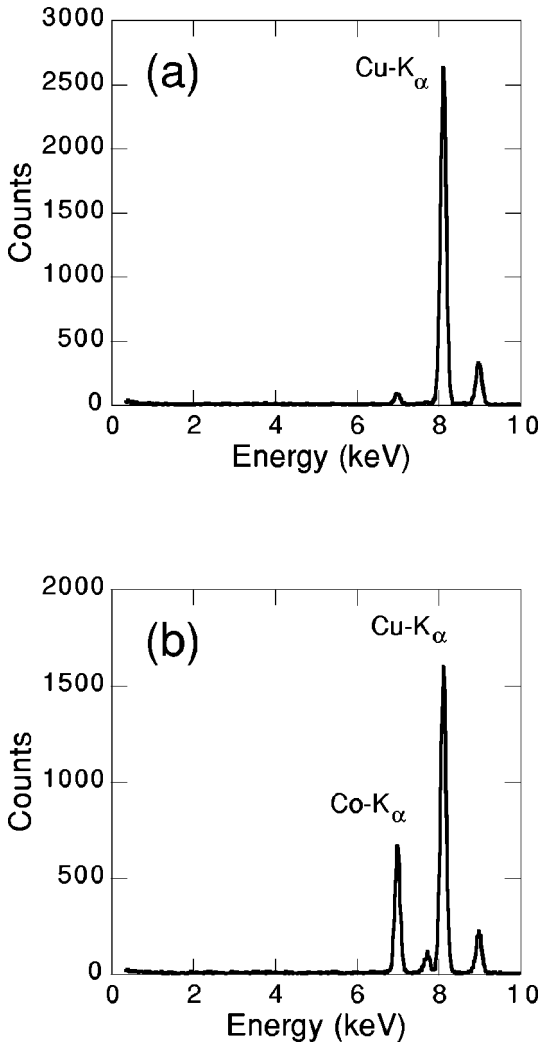

FIG. 3. EDS spectra of (a) intragrain zone and (b) one of the particles observed at the grain boundaries (γ phase), showing the Cu and Co characteristic x rays.

the in-phase component $\chi'(T)$ shows only one maximum, which broadens and shifts to higher temperatures as the annealing time t_a is increased. The out-of-phase component $\chi''(T)$ also shows maxima accompanying the $\chi'(T)$ peaks but located at a slightly lower temperature. The location in temperature of the $\chi'(T)$ and $\chi''(T)$ susceptibility peaks due to the blocking transition of a particle assembly depends, in general, on the particle anisotropy energy and thus on the particle volume.[24] In the context of a noninteracting particle assembly model, equation (A2) relates the particle size and the blocking temperature. If the temperature at the maximum of $\chi''(T)$ is taken as a rough estimate of the blocking temperature, and if an anisotropy constant for fcc cobalt of 8.9×10^4 J/m^3 is assumed, this expression yields a particle diameter of 6.0 nm for the sample in the $25h^*$ state, which is in agreement with the TEM observations. Previous works on $Cu_{90}Co_{10}$ alloys have shown that the mean size of the β-phase particles increases with the severity of the thermal treatments.[19,25,26] Therefore, if the $\chi(T)$ susceptibility peaks were due to the blocking transition of the β-phase particles,

they will be shifted to higher temperatures as t_a and, thus, the particle sizes, are increased. Indeed, this effect is quite apparent in Fig. 4.

Between 200 and 300 K, χ'' is almost temperature independent. We have fit the experimental data to a temperature-independent contribution shown in Table I. We believe this contribution is due to the γ-phase precipitates whose approximate value χ''_γ is observed to increase with t_a. It should also be noted that the $\chi''(T)$ curves of the sample in both, the $25h^*$ and $25h$ states, are slightly different. The migration of the Co atoms to the grain boundaries, even at room temperature, could explain the small differences between both curves. This mechanism also explains the nonzero $\chi''(T)$ in the whole temperature range, as previously detected in the other $Cu_{100-x}Co_x$ alloy.[19,26]

Figure 5 shows the field dependence of the magnetization, measured at 300 K, for the as-quenched, $6h$ and $25h^*$ states. As the annealing time is increased, saturation is achieved at gradually lower values of applied field. On annealing, there is also a strong increase in the remanence (3.7, 7.1, and 8.9 $A\,m^2/kg$ Co, respectively). These facts lead to the increase of the hysteresis loop area (not shown) observed after thermal treatments.

As a rough approximation, we have fitted the $M(H)$ curve of the $25h^*$ state by a single Langevin function plus a field-independent contribution (solid line in Fig. 5). This estimation is based on the evidence, supported by the TEM micrographs, of β and γ phases in the $25h^*$ state (Sec. III A). Using the room-temperature value of the spontaneous magnetization for bulk fcc cobalt, $M_s = 164.8\ A\,m^2/kg$, the best fit has been obtained for a particle size of 5.3 ± 0.1 nm. The value resulting from this estimation is also in agreement with the TEM results.

Plots of the magnetization as a function of H/T for the sample in the same states (not shown) did not superimpose at any temperature. The failing of this typical test of the superparamagnetic behavior agrees with the TEM experiments in that this sample, in any of its states, cannot be considered as a *mere assembly* of superparamagnetic particles.

In summary, both TEM experiments and magnetic characterization results confirm that the microstructural hypotheses proposed in Sec. I apply well to the sample studied in this paper.

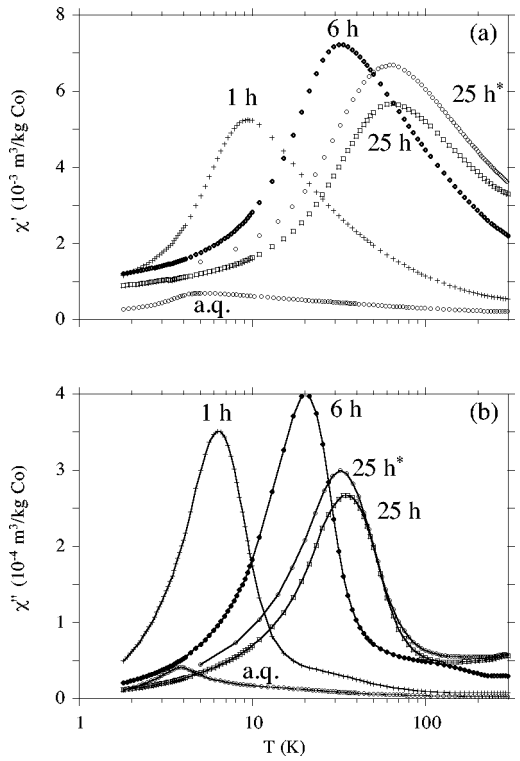

FIG. 4. Temperature dependence of the in-phase (a) and out-of-phase (b) components of the susceptibility measured at 10 Hz for the $Cu_{97.5}Co_{2.5}$ as-quenched sample, and for the same sample subsequently annealed at 550 °C during 1, 6, 25 h. Eventually, the sample has been kept at room temperature on a shelf for 19 months and, at the end of this time period, it has been characterized again; the corresponding results are labeled $25h^*$. The solid lines in (b) are only a guide for the eye.

IV. DISCUSSION

A. The frequency dependence of the dynamical susceptibility

For an ensemble of noninteracting magnetic particles in the superparamagnetic range, the over-barrier rotation of the particle magnetic moment is a thermally activated process with an associated characteristic time that can be described by an Arrhenius law. At low enough frequencies (up to kilohertz) the experimental χ'' data, expressed as a function of the variable $T\ln(\omega\tau_0)$, must collapse into a master curve,[24] having the τ_0 factor value between 10^{-9} and 10^{-11} s, depending on the magnetic ordering into the particles[27] (see the Appendix). The occurrence of interactions usually gives rise to a weaker frequency dependence of the location of the $\chi''(T)$ maximum, $T_{max}(\omega)$, than in the noninteracting case. If we insist on using an Arrhenius-type law when interactions exist, we generally obtain unphysically small τ_0 values.[28]

The above-described $\chi''(T)$ scaling has been applied to our system, as shown in Fig. 6. The preexponential factors estimated by this method are shown in Table I. The most interesting feature in Fig. 6 is the change in the frequency dependence of the $\chi''(T)$ curve with the thermal treatment. For the as-quenched sample, the $\chi''(T)$ peak shows a very sharp cusp and a frequency dependence which resemble that of spin glasses. The thermal treatment smoothes this peak and gradually changes its frequency dependence into a typical superparamagnetic blocking peak one.

A quantitative estimate of the frequency dependence of $T_{max}(\omega)$ can also be obtained from the ratio $\Delta T_{max}/T_{max}\Delta\log_{10}\nu$ (see the Appendix). This phenomenological parameter has previously been used as a criterion to compare a wide variety of disordered magnetic systems.[4,29] This quantity decreases for stronger magnetic interactions. In Table I we have included the values of this parameter for the different annealing times used. It should be noted that the value obtained for the sample $25h^*$ (~ 0.1) is in agreement with those calculated for systems of noninteracting particles (see the Appendix). However, the value obtained for the as-

TABLE I. Comparison of the γ-phase contributions χ''_γ and the frequency shift, $\Delta T_{max}/T_{max}\Delta \log_{10}\nu$ (calculated at $\nu=1$ Hz) for the $Cu_{97.5}Co_{2.5}$ as-quenched, $1h$, $6h$, $25h$, and $25h^*$ states. The best fit of the experimental $\chi''[T \ln(\omega\tau_0)]$ data has been used to obtain τ_0 for the same cases. The calculated values for a noninteracting fine particle system has also been included.

t_a (h)	χ''_γ (10^{-5} m^3/kg Co)	$\Delta T_{max}/T_{max}\Delta \log_{10}\nu$	τ_0 (s)
a.q.	0.3 ± 0.1	0.04	10^{-22}
1	0.7 ± 0.1	0.09	10^{-13}
6	3.1 ± 0.2	0.11	10^{-12}
25	4.8 ± 0.5	0.12	10^{-11}
25*	5.5 ± 0.5	0.12	10^{-11}
Noninteracting fine particle systems		0.10–0.12	10^{-9}–10^{-11}

quenched sample is greater than those observed for canonical spin glasses (<0.02) but smaller than values typically obtained for dilute magnetic semiconductors (~0.06).[3] For interacting particle systems, this parameter can vary in a very wide range of values depending on the concentration and the nature of the particles.[4] From data shown in Table I we can see that the variations of both, the τ_0 and the $\Delta T_{max}/T_{max}\Delta\log_{10}\nu$ values with t_a, are consistent with the hypothesis that thermal treatments produce a gradual change from a spin-glass-like to a typical superparamagnetic behavior. This result suggests a basic question: What type of magnetic interaction may be at the origin of such behavior?

In Ref. 30 Mørup suggested that the ordering temperature of a system that consists of randomly distributed particles interacting via dipolar interactions can be estimated by

$$T_{dip}\sim \alpha_0(\mu_0/4\pi)(m^2/k_B a^3), \tag{4.1}$$

where a is a measure of the mean distance between pairs of dipole moments, m is the mean magnetic dipole moment and α_0 is a constant with a value of the order of unity. For an assembly of ferromagnetic particles a good estimation for m^2/a^3 is $M_s^2 V\epsilon$, M_s being the spontaneous magnetization, V being the average particle volume, and ϵ being the fraction of the total volume occupied by particles. The magnitude of the dipole-dipole interaction can therefore be estimated from $T_{dip}=(\mu_0/4\pi k_B)M_s^2 V\epsilon$ (Ref. 5). Although this expression does not take into account the actual configuration of the particle ensemble, since all our samples can be considered as containing randomly arranged particles, one can use it for understanding the net effect of the thermal treatment on the

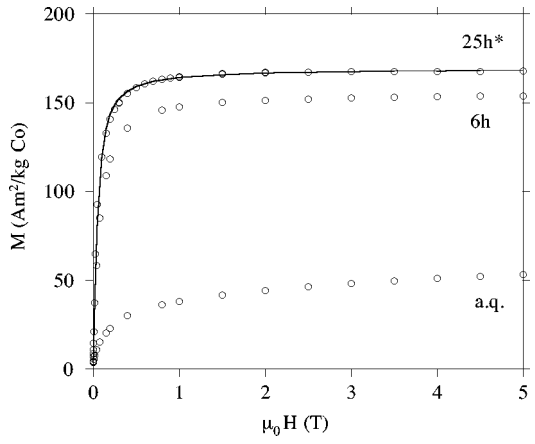

FIG. 5. Magnetization curves measured at 300 K of the sample in the as-quenched, $6h$ and $25h^*$ states. The solid line is the fit by a single Langevin function plus a field-independent contribution.

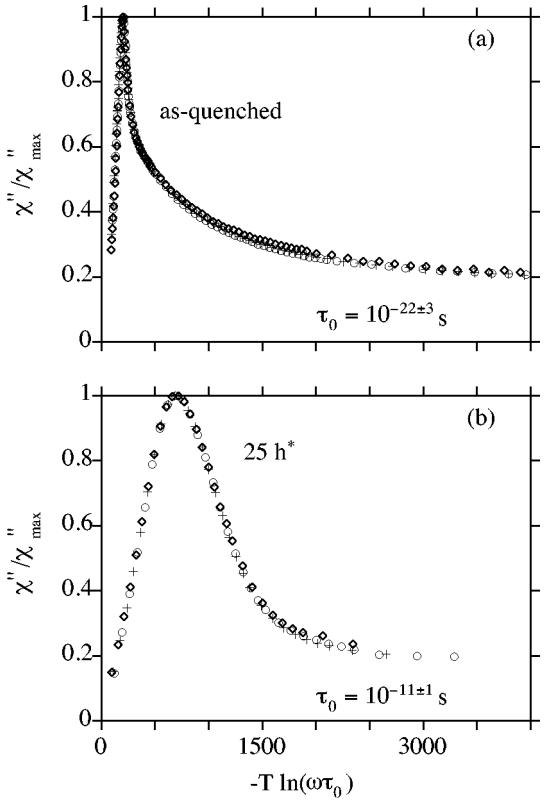

FIG. 6. Normalized out-of-phase susceptibility plotted against $T\ln(\omega\tau_0)$ at 1 Hz (circles), 10 Hz (crosses), and 120 Hz (diamonds), for $Cu_{97.5}Co_{2.5}$ in the as-quenched (a) and the $25h^*$ states (b). Note that the preexponential factor estimated from (b) is typical of noninteracting particle assemblies, whereas the unphysical value obtained from (a) suggests a different origin (see text).

dipole-dipole interaction energy.

When precipitation starts to occur, both V and ϵ parameters increase as a consequence of the diffusive flux of solute atoms from the matrix to the precipitates. Once the precipitation reaction is completed, the growth of the large particles occurs at the expense of the small particles due to the coarsening reaction. Along this process the volume fraction occupied by particles does not change. Early studies on $Cu_{100-x}Co_x$ alloys ($x=2.0$–2.7) that included TEM and field ion microscopy experiments support this hypothesis.[25,31] Therefore, an increase of T_{dip} with t_a would be expected at both stages. It is known, from magnetic studies on ferrofluids,[28] that if the only relevant interparticle interaction present in the system is of dipolar type an increase in the so calculated T_{dip} value accompanies a reduction in the frequency dependence of T_{max}. Our results for the frequency dependence of T_{max} (Table I) show the opposite trend, suggesting that the leading type of interaction cannot be of dipole-dipole type.

B. The role of the α phase and the consequences of the β-phase particle growth

It is commonly assumed, and occasionally stated, that the Co-rich particle precipitates are surrounded by a pure Cu matrix. This might appear reasonable in view of the great driving force for precipitation and the relatively long annealing times used for the earlier studies on these alloys. However, the development of rapid solidification methods makes it necessary to consider stages during which the Co content of the fcc Cu-Co supersaturated solid solution (α phase) is still significant.

We believe that the consideration of the α phase is crucial in understanding the nature of the interparticle interactions in these systems. In noble-metal/3d transition-metal alloys (e.g., Cu-Mn), the dominant interaction between spins is known to be of RKKY type.[3] The Cu-Co alloy naturally belongs to this class of materials. In addition, the low solubility of cobalt in copper at room temperature[7] also generates a variable amount of cobalt-rich precipitates that also interact via RKKY interaction.[32] In this scenario, and also obeying the natural decay of the RKKY interaction upon distance between magnetic moments, it appears logical to consider that the interparticle interactions are enhanced by the presence of intermediate cobalt spins (α-phase).

Hattenhauer and Haasen investigated the decomposition of a $Cu_{99}Co_1$ alloy annealed at 550 °C during different times by using bright-field/zone-axis TEM.[33] These authors performed a quantitative analysis of the relative distances between the β-phase precipitates and they observed a decrease in the mean number of particles at distances smaller than 10 nm. This behavior was explained by the existence of depleted zones surrounding the precipitates, as shown in Fig. 7.

From the magnetic and microstructural considerations made above, it follows that, in the annealing process, the cobalt depletion of the surroundings of the β-phase particles leads to the magnetic decoupling of this phase from the rest of the matrix. We estimate that, for a completely Co-depleted shell ~25–50 Å thick, (~8–14 Cu lattice parameters), the decay of the RKKY interaction strength may become so important that the particle magnetic moment and the surrounding matrix might become effectively uncoupled. We define η as the effective thickness of the Co-depleted shell if a total depletion is assumed. It should be noted that this parameter is a lower limit to the real thickness of the shell whose concentration of cobalt is actually affected by the particle growth. In practice, it appears logical that η be dependent on the particle size and on the cobalt concentration of the alloy. For a given particle size, the lower the cobalt concentration of the matrix is, the longer η should be in order to *drain* enough Co atoms to form the particle. Conversely, for a given cobalt concentration, the larger the particle is, the longer η should be for the same reason.

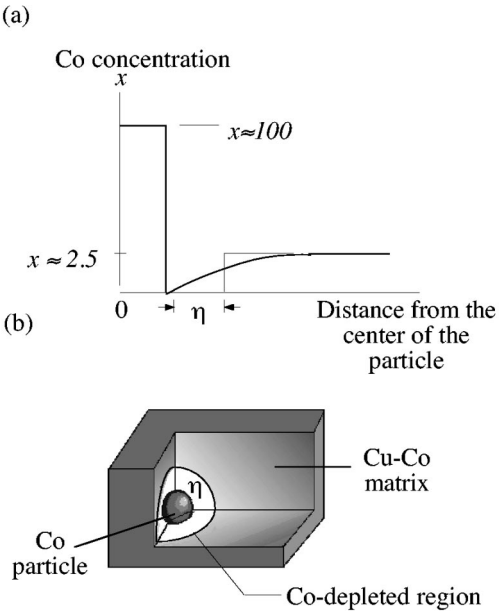

FIG. 7. (a) Schematic diagram of the proposed Co-concentration profile around a Co-rich particle precipitated in Cu-Co matrix. The horizontal axis represents the distance measured from the centre of the particle. The parameter η is the effective thickness of the Co-depleted shell if a total depletion is assumed. (b) Three-dimensional representation of the same phenomenon.

It should be noted that the magnetic coupling between the β-phase particles depends dramatically on the cobalt content of the fcc Cu-Co supersaturated solid solution (α phase). The mechanism accounts in a natural way for the relationship between the size of the particle and the strength of interactions and poses a number of interesting (and fulfilled) predictions.

(i) It may be possible to obtain a noninteracting ensemble of particles diluted in a Cu-Co matrix if the particles are large enough to be magnetically isolated from the α phase, provided they are separated by sufficiently long distances so as to keep low the dipolar interaction strength (Sec. IV C).

(ii) The β-phase particles might undergo a change in the dominant coupling mechanism due to their own growth process (Sec. IV D).

(iii) Finally, if the Co-depletion process extends to a sufficiently long period of time, one can reasonably expect that the Co-depleted shells will become in mutual contact, leading to the existence of different magnetically uncoupled α-phase regions (Sec. IV E).

C. A noninteracting ensemble of Co particles in a Cu-Co matrix

In order to corroborate whether or not it is possible to obtain a noninteracting ensemble of Co-rich particles diluted in a Cu-Co matrix, we have looked at the published literature on these alloys. Bitoh *et al.*[34] studied molten $Cu_{97}Co_3$ alloy sucked into a quartz tube and solidified into a rod by quenching in ice water. The reported sample dimensions and the quenching method used, clearly suggest an effective cooling rate much slower than that of our melt-spun sample. This procedure leads to the growth of large spherical precipitates of Co ($\sim$6.7 nm) which, according to a simple calculation would be surrounded by a Co-depleted shell of $\eta \sim 8$ nm. This is consistent with the typical superparamagnetic behavior observed in that material. It should also be noted that Cu-Co alloys synthesized by methods similar to that of Bitoh *et al.* have been used to study basic properties of superparamagnetism over the past 40 years.[12] In our previous work,[21] the relaxational behavior of a fraction of the Co-rich particles shows a magnetic behavior typical of a noninteracting assembly of particles, also according to the hypothesis described in Sec. IV B.

D. Change in the dominant coupling mechanism

The β-phase particles might undergo a change in the dominant coupling mechanism due to the nature of the growth process. Two magnetic *regimes* might appear: (i) when the β-phase particles are small enough, they might be coupled via the α phase (RKKY interaction) and, (ii) as soon as these particles become larger, their own growth would cause uncoupling between these particles and the surrounding α phase.

This behavior is consistent with the thermal evolution of the out-of-phase susceptibility for a set of $Cu_{90}Co_{10}$ alloys previously studied.[19] For the as-quenched sample only one anomaly is visible in $\chi''(T)$ as shown in Fig. 5 of Ref. 19. However, after the thermal treatment, this anomaly splits into two different peaks, one due to the α-phase freezing and the other due to the blocking transition of the β-phase particles. According to the microstructural picture described in Sec. IV B (see Fig. 8), the existence of one or two anomalies in the $\chi''(T)$ curves should be strongly dependent on the size of the Co-rich particles and the nominal Co concentration of the alloy. In very dilute Cu-Co alloys, which is the case of the samples studied in this work, the peak due to the the α-phase freezing might lay outside the temperature window of the experiment, so only one peak would be visible.

We have estimated the magnitude of the dipolar interaction between the large Co-rich precipitates located at the grain boundaries (γ phase) and the neighboring β-phase particles. A simple calculation indicates that the dipolar energy between a Co precipitate of 50 nm and a particle of 6 nm, separated by a distance of 100 nm, is 8×10^{-22} J. This value is one order of magnitude less than the anisotropy barrier energy of such small particle, which comes out to be 8×10^{-21} J if an anisotropy constant of 8.9×10^4 J/m^3 is assumed. This estimate suggests that the magnetic relaxation dynamics of the β-phase particles located at a distance larger than $\sim$100 nm, as it is the general case given the size of the crystalline grains $\sim 1-2$ μm, should be affected little by this interaction. The contribution of particles at smaller distances would be substantially reduced due to the known existence of precipitated free zones adjacent to the grain boundaries.[35]

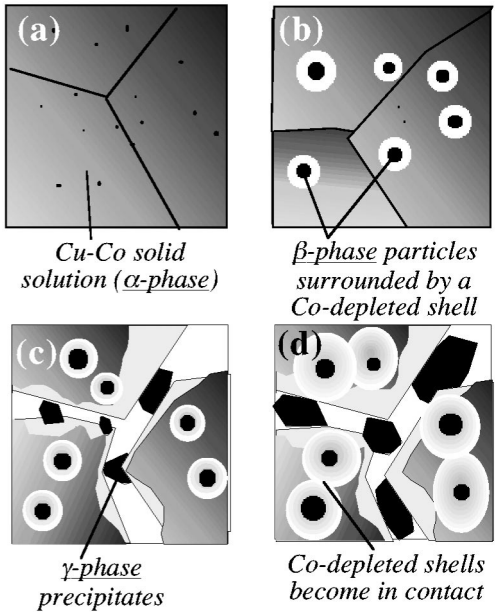

FIG. 8. Illustration of the proposed Co-rich particle growth process, for a Cu-Co sample at the as-quenched state (a), and for the same sample after sequential annealing treatments (b), (c), and (d).

The occurrence of two distinct susceptibility anomalies as separate phenomena in the same system has scarcely been observed, although it has been detected in $Eu_xSr_{1-x}S$ for $x < 0.1$ (Ref. 36). Not free of controversies, the authors eventually ascribed the two anomalies to, apparently independent, magnetic blocking of large and small Eu clusters.[37] Later comments on the same experiments suggested that the two anomalies could exist independently due to the short-range nature of the intercluster interactions; furthermore, it was predicted that in other systems with long-range interactions both anomalies might not be resolved.[2] In fact, only the failure of the RKKY interaction mechanism, as explained in Sec. IV B, could explain the occurrence of two anomalies in Cu-Co alloys.

E. Intensified Co-depletion process

After a long enough period of time, the Co-depleted shells may reach mutual contact, producing different α-phase magnetically uncoupled regions (Fig. 8). This phenomenon would actually give rise to several spin-glass freezing temperatures, as previously suggested by data shown in Fig. 6(b) of Ref. 19 for the $Cu_{90}Co_{10}$ sample annealed at 620 °C.

V. CONCLUSIONS

We have carefully analyzed the dynamical susceptibility and the field-dependent magnetization, together with a TEM microstructural characterization, of an originally melt-spun Cu-Co alloy with the aim of attaining a deeper understanding of the relationship between the microstructure and its magnetic properties. Contrary to most of the previous studies on this alloy, finer microstructural details beyond the mere existence of cobalt-rich nanoparticles are specifically considered in this paper. The magnetic relaxation observed in the as-quenched alloy is indicative of typical spin-glass-like dynamics. As far as the annealing time increases, this dynamics is gradually better described in terms of what is expected for a noninteracting particle ensemble. The process of particle growth seems to have a dramatic effect on the effectiveness of the RKKY interaction due to the Co depletion of the shell that surrounds each particle. As a consequence of this, the largest particles become uncoupled (from a magnetic point of view) from the rest of the alloy and the dipole-dipole interaction, which is always present, appears not to be strong enough to produce a collective magnetic behavior.

In some cases, as the Co depletion proceeds, and provided the freezing temperature of the now uncoupled remaining spin-glass-like phase is high enough, two anomalies in both $\chi'(T)$ and $\chi''(T)$ are observed.[19] The results obtained come into the frame of early discussions about the similarities between spin glasses and superparamagnets.[38] A detailed comprehension of the microstructure seems to be of central importance to explain the nature of the competing interactions in real alloys. If we restrict ourselves to binary combinations of $3d$ transition metals with Cu, Ag, and Au, one can observe that those showing high solubility (for instance, CuMn or AuFe) are just the well-studied canonical spin glasses. However, in the cases of little solubility, rather good solid solutions can also be prepared by very fast cooling methods, although there is always a strong tendency to segregate nanometric precipitates conforming the so-called granular alloys. In Cu-Co alloys, a local effect at the nanometric scale, that is, the occurrence of Co-depleted zones surrounding the precipitates, appears capable of switching the magnetic behavior from the first case (a spin-glass) to the second (a granular alloy).

ACKNOWLEDGMENTS

The authors would like to acknowledge Rittmar von Helmolt for providing the samples studied in this work. We are also grateful to J. L. García-Palacios for his helpful discussions and suggestions to improve this paper. Spanish DGESIC under project PB98-1606 is also acknowledged.

APPENDIX

This appendix includes a number of useful results obtained in Refs. 24 and 39 as revised in Ref. 40.

At moderate and low frequencies ($\omega < 10^6$ Hz), the response to the transverse component of the probing field of a monodispersed ensemble of noninteracting magnetic particles with their anisotropy axis distributed at random is nearly the static response ($\tau_\perp \simeq 0$).[41] The longitudinal response $\tau_\parallel$ is mainly determined by the rotations of their magnetic moments over the potential barrier. For moderately high values of the potential barrier, this thermally activated process can be described by means of the Arrhenius law,

$$\tau_\parallel = \tau_0 \exp(Kv/k_B T), \tag{A1}$$

where K is the effective anisotropy constant, v is the volume of the particle, k_B is the Boltzmann constant, T is the temperature, and typically $\tau_0 \simeq 10^{-9} - 10^{-11}$ s. The diameter at which $\omega\tau_\parallel = 1$ is called *the blocking diameter*,

$$D_b = -[(6k_B T/\pi K)\ln(\omega\tau_0)]^{1/3}. \tag{A2}$$

We shall consider a solid dispersion of noninteracting single-domain magnetic particles with uniaxial magnetic anisotropy. We shall restrict our attention to particle assemblies that have their anisotropy axes oriented at random and an anisotropy constant that is the same for each particle. After these conditions, the in-phase susceptibility can be written as

$$\chi' = \frac{\pi}{6}\frac{\mu_0 \epsilon M_s^2}{3k_B T}\left(\int_0^{D_b} dD f(D) D^3 + \int_{D_b}^{\infty} dD\, f(D) D^3 \frac{\mathcal{R} - \mathcal{R}'}{\mathcal{R}} \right), \tag{A3}$$

where ϵ is the fraction of the total volume occupied by the particle ensemble, M_s is the spontaneous magnetization, and $f(D)dD$ is the fraction of volume occupied by particles with diameters between D and $D+dD$.[39] The functions $\mathcal{R}$ and its derivative $\mathcal{R}'$ are defined as (Ref. 24)

$$\mathcal{R} = \int_0^1 dx \exp(\sigma x^2) \tag{A4}$$

and

$$\mathcal{R}' = \int_0^1 dx\, x^2 \exp(\sigma x^2), \tag{A5}$$

where $\sigma = Kv/k_B T$. It should be noted that the first term in Eq. (A3) is the contribution of the superparamagnetic particles to the equilibrium linear susceptibility, whereas the second term is the contribution of the blocked particles. We can also get an approximate expression for the out-of-phase susceptibility

$$\chi'' = \frac{\pi}{18}\frac{\mu_0 \epsilon M_s^2}{K}\frac{\mathcal{R}'(\sigma_b)}{\mathcal{R}(\sigma_b)} f(D_b) D_b, \tag{A6}$$

where D_b is defined in Eq. (A2), and

$$\sigma_b = -\ln(\omega\tau_0). \tag{A7}$$

Equation (A6) reveals that $\chi''(T,\omega)$, unlike $\chi'(T,\omega)$, is nearly proportional to $f(D)$ and this implies that, for a given particle size distribution, the experimental $[\mathcal{R}(\sigma_b)/\mathcal{R}'(\sigma_b)]\chi''(T,w)$ data expressed as a function of the variable $-T\ln(\omega\tau_0)$ must collapse onto a single master curve. Hence, the search for optimum collapsing of the χ''

data can be used to determine τ_0. We use the term *nearly proportional* because the factor $\mathcal{R}'(\sigma_b)/\mathcal{R}(\sigma_b)$ depends in fact on T via τ_0. However, for frequencies up to the kilohertz range this dependence is very weak and the scaling relation is valid also for the $\chi''[-T\ln(\omega\tau_0)]$ curves.

The existence of a particle size distribution can be taken into account by averaging the blocking temperature over the full particle size distribution. The averaged blocking temperature $\overline{T_b}$ depends on the shape of the particle size distribution and, in general, it is related to the position of the $\chi''(T)$ maximum, $T_{\max}$. For multimodal distributions $\chi''(T)$ may even have several maxima. To find the explicit relation between $\overline{T_b}$ and $T_{\max}$, we must apply the condition $\partial\chi''(T)/\partial T|_{T=T_{\max}}=0$ to Eq. (A6), and one obtains

$$\overline{T_b}=\kappa T_{\max};\quad \kappa=\begin{cases} e^{(9/2)\rho^2} & \text{(log-normal)} \\ \dfrac{(\beta+3)(\beta+2)}{(\beta+1)^2} & \text{(gamma)}, \end{cases} \tag{A8}$$

in the case of a particle-size distribution which is log normal

$$f(D)=\frac{D_m}{\sqrt{2\pi}\rho D}\exp\left(-\frac{[\ln(D/D_m)]^2}{2\rho^2}\right), \tag{A9}$$

or gamma

$$f(D)=\frac{1}{\Gamma(\beta+1)D_0}\left(\frac{D}{D_0}\right)^{\beta}\exp\left(-\frac{D}{D_0}\right), \tag{A10}$$

respectively, where β, D_0, ρ, and D_m are the parameters of the distributions, and Γ is the *gamma function*.

The relation $\overline{T_b}\propto T_{\max}$ can be justified for many types of size distribution.[42] Hence, we can analyze the frequency shift of the $\chi''(T)$ maximum to obtain conclusions about the validity of Eq. (A1) in a particular system.

The frequency dependence of $T_{\max}(\omega)$ can also be studied from the ratio $\Delta T_{\max}/T_{\max}\Delta\log_{10}\nu$. For noninteracting fine particles, this ratio can be estimated from equations (A2) and (A8), namely,

$$\frac{1}{T_{\max}}\frac{\partial T_{\max}}{\partial\log_{10}\nu}=-\frac{1}{\ln(\omega\tau_0)}\underbrace{\frac{\partial\ln(\omega\tau_0)}{\partial\log_{10}\nu}}_{\ln 10}. \tag{A11}$$

If we assume that $\tau_0\sim10^{-9}$–10^{-11} s and $\nu=1$ Hz, the value of expression (A11) yields $\sim$0.10–0.12.

It should be noted that the use of $\Delta T_{\max}/T_{\max}$ per decade of frequency, when $\chi''(T)$ just shows a single maximum, seems useful but its physical grounds are already included in the more complete $\chi''[T\ln(\omega\tau_0)]$ scaling, which applies even in the case of multimodal particle size distributions. We have included the former in order to compare our results with the results that appear in the spin-glass literature.

*Present address: Conservatoire National des Arts et Métiers (CNAM), Salesianos-Zaragoza, 50009 Zaragoza, Spain. Electronic address: alopezpo@navegalia.com

[1] A. López, F. J. Lázaro, J. L. García-Palacios, A. Larrea, Q. A. Pankhurst, C. Martínez, and A. Corma, J. Mater. Res. **12**, 1519 (1997).
[2] K. Binder and A. P. Young, Rev. Mod. Phys. **58**, 801 (1986).
[3] J. A. Mydosh, *Spin Glasses: An Experimental Introduction* (Taylor & Francis, London, 1993).
[4] J. Dormann, D. Fiorani, and E. Tronc, J. Magn. Magn. Mater. **202**, 251 (1999).
[5] T. Jonsson, P. Nordblad, and P. Svedlindh, Phys. Rev. B **57**, 497 (1998).
[6] T. Jonsson, J. Mattsson, C. Djurberg, F. A. Khan, P. Nordblad, and P. Svedlindh, Phys. Rev. Lett. **75**, 4138 (1995).
[7] M. Hasebe and T. Nishizawa, CALPHAD: Comput. Coupling Phase Diagrams Thermochem. **4**, 83 (1980).
[8] J. R. Childress and C. L. Chien, Phys. Rev. B **43**, 8089 (1991).
[9] J. Wecker, R. von Helmolt, K. Samwer, and L. Schultz, Appl. Phys. Lett. **62**, 1985 (1993).
[10] I. S. Servi and D. Turnbull, Acta Metall. **14**, 161 (1966).
[11] W. Wagner, J. Piller, H. P. Degischer, and H. Wollenberger, Z. Metallkd. **76**, 693 (1985); R. Busch, F. Gärtner, C. Borchers, P. Haasen, and R. Bormann, Acta Metall. Mater. **43**, 3467 (1995).
[12] J. Becker, Trans. AIME **209**, 59 (1957); C. P. Bean and J. D. Livingston, J. Appl. Phys. **30**, 120 (1959).
[13] K. Krop, J. Korecki, J. Żukrowski, and W. Karaś, Int. J. Magn. **6**, 19 (1974); J. Korecki and K. Krop, Surf. Sci. **106**, 444 (1980).
[14] T. Bitoh, K. Ohba, M. Takamatsu, T. Shirane, and S. Chikazawa, J. Phys. Soc. Jpn. **64**, 1311 (1995).
[15] A. E. Berkowitz, J. R. Mitchell, M. J. Carey, A. P. Young, S. Zhang, F. E. Spada, F. T. Parker, A. Hutten, and G. Thomas, Phys. Rev. Lett. **68**, 3745 (1992); J. Q. Xiao, J. S. Jiang, and C. L. Chien, *ibid.* **68**, 3749 (1992).
[16] M. N. Baibich, M. G. M. Miranda, G. J. Bracho Rodríguez, A. B. Antunes, H. Rakoto, N. Negre, M. Goiran, J. M. Broto, E. F. Ferrari, F. C. S. da Silva, and M. Knobel, J. Magn. Magn. Mater. **196-197**, 45 (1999).
[17] B. J. Hickey, M. A. Howson, S. O. Musa, and N. Wiser, Phys. Rev. B **51**, 667 (1995).
[18] H. J. Blythe and V. M. Fedosyuk, J. Phys.: Condens. Matter **7**, 3461 (1995).
[19] A. López, F. J. Lázaro, R. von Helmolt, J. L. García-Palacios, J. Wecker, and H. Cerva, J. Magn. Magn. Mater. **187**, 221 (1998).
[20] B. Idzikowski, U. K. Rössler, D. Eckert, K. Nenkov, and K. H. Müller, Europhys. Lett. **45**, 714 (1999); P. Panissod, M. Malinowska, E. Jedryka, M. Wojcik, S. Nadolski, M. Knobel, and J. E. Schmidt, Phys. Rev. B **63**, 014408 (2000).
[21] A. López, F. J. Lázaro, and R. von Helmolt, J. Magn. Magn. Mater. **196-197**, 61 (1999).
[22] D. B. Williams and C. Barry Carter, *Transmission Electron Microscopy* (Plenum Press, New York, 1996).
[23] R. Hattenhauer and F. Haider, Scr. Metall. Mater. **25**, 1173 (1991).
[24] M. I. Shliomis and V. I. Stepanov, in *Relaxation Phenomena in Condensed Matter*, edited by W. Coffey, Vol. LXXXVII of Advances in Chemical Physics Series (Wiley, Amsterdam, 1994), p. 1.

[25] H. Wendt and P. Haasen, Scr. Metall. **19**, 1053 (1985).
[26] W. Wang, F. Zhu, W. Lai, J. Q. Wang, G. Yang, J. Zhu, and Z. Zhang, J. Phys. D **32**, 1990 (1999).
[27] T. Jonsson, J. Mattsson, P. Nordblad, and P. Svedlindh, J. Magn. Magn. Mater. **168**, 269 (1997).
[28] C. Djurberg, P. Svedlindh, P. Nordblad, M. F. Hansen, F. Bødker, and S. Mørup, Phys. Rev. Lett. **79**, 5154 (1997).
[29] J. L. Tholence, Physica B & C **126**, 157 (1984).
[30] S. Mørup, Europhys. Lett. **28**, 671 (1994).
[31] W. Wagner, J. Phys. F: Met. Phys. **16**, L239 (1986).
[32] G. M. Genkin and M. V. Sapozhnikov, Appl. Phys. Lett. **64**, 794 (1994); D. Altbir, J. d'Albuquerque e Castro, and P. Vargas, Phys. Rev. B **54**, R6823 (1996).
[33] R. Hattenhauer and P. Haasen, Philos. Mag. A **68**, 1195 (1993).
[34] T. Bitoh, K. Ohba, M. Takamatsu, T. Shirane, and S. Chikazawa, J. Phys. Soc. Jpn. **64**, 1305 (1993).
[35] J. W. Martin, *Micromechanisms in Particle-Hardened Alloys* (Cambridge University Press, Cambridge, 1980).
[36] G. Eiselt, J. Kötzler, H. Maletta, D. Stauffer, and K. Binder, Phys. Rev. B **19**, 2664 (1979).
[37] J. Kötzler and G. Eiselt, Phys. Rev. B **25**, 3207 (1982).
[38] K. H. Fischer and J. A. Hertz, *Spin Glasses* (Cambridge University Press, Cambridge, 1993).
[39] P. Svedlindh, T. Jonsson, and J. L. García-Palacios, J. Magn. Magn. Mater. **169**, 323 (1997).
[40] J. L. García-Palacios, Adv. Chem. Phys. **112**, 1 (2000).
[41] Y. I. Raĭkher and M. I. Shliomis, Zh. Eksp. Teor. Fiz. **67**, 1060 (1974) [Sov. Phys. JETP **40**, 526 (1975)].
[42] J. I. Gittleman, B. Abeles, and S. Bozowski, Phys. Rev. B **9**, 3891 (1974).